Electronic Supplementary Information

Remotely powered distributed microfluidic pumps and mixers based on miniature diodes

Suk Tai Chang, Erin Beaumont, Dimiter N. Petsev and Orlin D. Velev*

*E-mail: odvelev@unity.ncsu.edu

Supplementary Movies

Supplementary Movie "M1_Flow_Between_Diodes_Low_Field.wmv"
Reverse electroosmotic flow is generated between the two diodes facing in the same direction on the sides of the microchannel under the external AC field of 30 V cm^{-1} and 1 kHz.

Supplementary Movie "M2_Flow_Between_Diodes_High_Field.wmv"
More intense flow is created between the two diodes with the same orientation at a higher external AC field of 60 V cm^{-1} and 1 kHz.

Supplementary Movie "M3_Flow_Pumped_Corner_Channel.wmv"
The fluid motion at the corner of the closed rectangular-loop channel confirms the one-directional circulation driven by the diodes. Time lapse images of the tracer particles were acquired at the left, upper corner of the Figure 1a with a 1 second interval between the frames. Movie is speeded 2X. The magnitude of the external AC field was 60 V cm^{-1} with 1 kHz.

Supplementary Movie "M4_Diode_Mixer.wmv"
Microfluidic mixing by oppositely facing diodes embedded in the channel walls. Milli-Q water (top flow in the channel) and Texas Red fluorescent dye solution (bottom flow) were driven by a syringe pumps with 2 μL min^{-1} flow rate from the left to right in the movie. The external AC field applied was 133 V cm^{-1} at 1 kHz. The movie was recorded using a digital camera attached to the confocal microscope. The total recoding time was 74 seconds. Movie is speeded 3X.

Supplementary Movie "M5_Simulation_Mixing_Whole_Channel.wmv"
Numerical simulation for flow profiles and concentration distributions in the whole channel verifies the enhancement data for diode mixing of the two laminar flows. The pressure-driven flow rates for water (top half of the channel) and the dye solution (bottom flow) were 2 μL min^{-1} each. The zeta potential, ζ, of the diode surfaces was set at +60 mV and the external AC field was set to 133 V cm^{-1}.

Supplementary Movie "M6_Simulation_Mixing_Diode_Mixer.wmv"
Zoom in on the result of the simulation inside the diode mixer microchamber confirms the generation of the transverse flow across the interface between the two laminar streams from the miniature diodes.

Supplementary figures

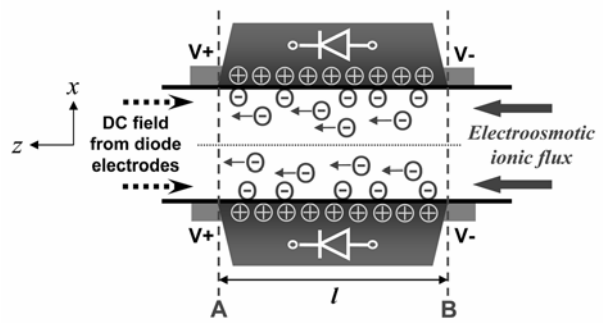

Figure S1. Schematic illustration of the localized electroosmotic flow for the pumping in a microchannel with a pair of diodes oriented in the same direction in low pH solutions. The charge at the diode surface results in the formation of an electric double layer. When AC field is applied, the diode shortens the field in one direction and behaves as a near dielectric object in the other.

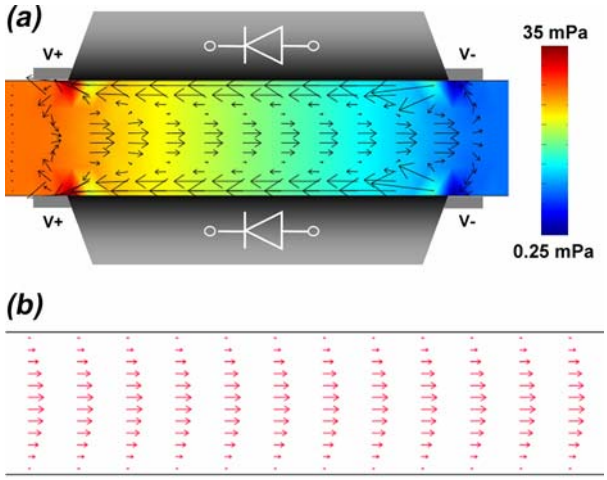

Figure S2. Flow simulation for the diode pump in the closed rectangular microchannels with embedded diodes using COMSOL software. (a) Computed velocity profiles between the parallel oriented diodes at the channel walls. The velocity vector magnitudes are represented by the lengths of the arrows. Colours show the pressure. (b) Computed velocity profiles for the fluid flow pumped by the diodes in the middle of longer channel without diodes. The direction of the circular flow in the rectangular loop microchannel is the same as the electroosmotic flow on the diode surfaces. The length of the arrows for the velocity magnitude in (b) is magnified for better visualization.

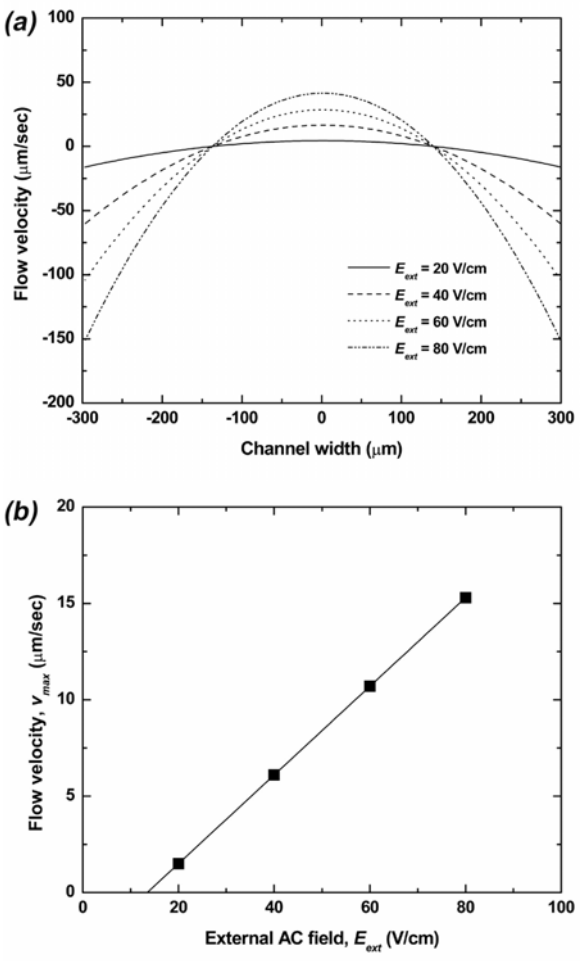

Figure S3. Numerical simulations for the diode pumping in the closed rectangular microchannel. (a) Velocity of the reverse electroosmotic flow between two diodes on the channel walls as a function of the channel width. As the external AC field increases, the electroosmotic flux (negative velocity) on the diode surfaces and the backflow (positive velocity) in the middle of the channel become larger, which match well the experimental observations. (b) Velocity of the flow in the centre of the channel loop without the diodes as a function of the external electric field. The simulation data verify the ability of the diodes on the microchannel to pump liquids through the channel with a linear dependence on the AC field. The simulation results show a good correlation with the experimental data and support the electroosmotic pumping mechanism.

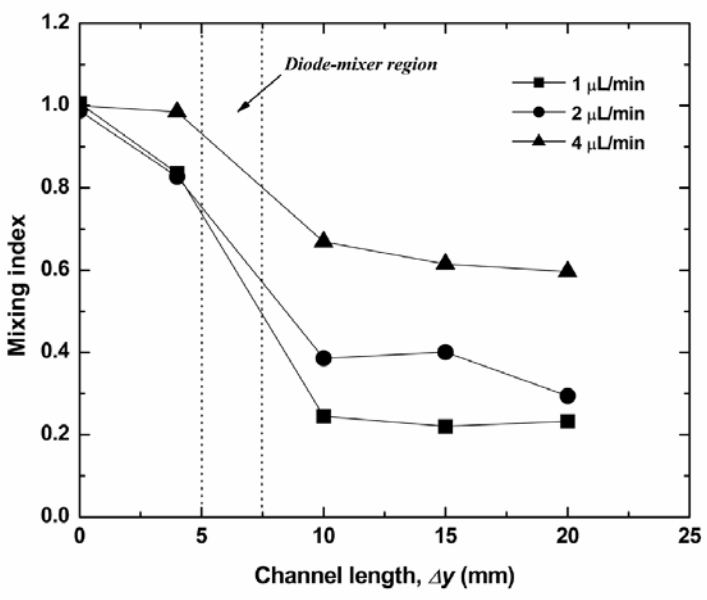

Figure S4. Mixing index at various pressure-driven flow rates as a function of the distance from the Y-shaped channel junction. Water and fluorescent dye solution were adjusted to ~ pH 5.4. The AC external field was 133 V cm^{-1} at 1 kHz. As the flow speed was increased, lower degree of mixing efficiency was observed. Mixing at high flow velocities could be performed with a series of diode mixers in the channel.

Numerical Simulation Details

Numerical simulation of fluid flows in diode pumping

We solved using the FEMLAB package the continuity and Navier-Stokes equations for fluid motion in the diode pumping system,

$$\nabla \cdot \mathbf{V} = 0 \tag{S1}$$

$$\frac{\partial \mathbf{V}}{\partial t} + \mathbf{V} \cdot \nabla \mathbf{V} + \frac{1}{\rho} \nabla P = \nu \nabla^2 \mathbf{V} \tag{S2}$$

where $\mathbf{V}$ is the velocity vector, ρ is the density of liquid, P is the pressure, ν is the kinematic viscosity. The Debye length, used as characteristic thickness of electric double layer in the electrolyte solution, is ~ 100 nm, which is much smaller than the length scale of the microchannel. Therefore, the electric double layer thickness can be neglected in the simulation domain. The electroosmotic flow velocity in equation (2) was used as a liquid slip boundary condition on the diode surface for the numerical calculations,[38,39] while no-slip condition was applied at the channel walls beyond the diodes. The dielectric permittivity and hydrodynamic properties of water were $\varepsilon = 80$, $\rho = 1000$ kg m^{-3} and $\mu = 10^{-3}$ kg m^{-1} s^{-1}. The zeta potential at the diodes surfaces was +60 mV. The rest of the channel (apart from the diode region) is not subject

to directional electric field and hence does not contribute to the electroosmotic driving force, although it contributes to the overall hydrodynamic resistance.

The electric field inside the channel for calculating the electroosmotic flow at the diode surfaces was simulated during the positive half-cycle of the applied AC voltage, because the diode acts as a conductor during the other cycle. The electric potential distribution in the rectangular channel domain was calculated using the Poisson equation,

$$\nabla^2 \phi = -\frac{\rho_e}{\varepsilon_0 \varepsilon} \tag{S3}$$

where ϕ is the electric potential and ρ_e is the electric charge density. The rectified electric potentials on the diode electrodes were provided by the experimental data in our previous work.[44] We assume that the physical properties of the fluids were uniform in the whole microchannel domain during the field application. A steady state flow is assumed in equation (S2), which is reasonable for the low *Re* regimes that correspond to our experiment.[39,40]

Numerical simulation of diode mixing

The fluid flow was determined by solving equations (S1), (S2) and (S3) together and the obtained fluid flow field was then introduced into the convective diffusion equation,

$$\frac{\partial c}{\partial t} + \mathbf{V} \cdot \nabla c = \nabla \cdot (D \nabla c) \tag{S4}$$

where c is the concentration and D is the diffusion coefficient.

The slip boundary condition on the diode surfaces was also used in the numerical calculations because the thickness scale of the electric double layer is negligible compared to the characteristic length of the Y-shaped channel. The same inflow velocity as the experiment (2 μL min^{-1}) was defined at the two inlets. The electric conditions in the simulations were applied in the same way as in the diode pumping simulations, except for defining the polarity of the rectified electric potential at the diode electrodes in opposite directions. The concentrations at the upper and lower inlets in the simulation domain were assigned as $c = 0$ and $c = 1$, respectively. After a conformal triangular mesh was formed by the software for the domain, the time-dependent solver mode was used.